doi: 10.3969/j.issn.0490-6756.2018.05.027

电化学表面处理和 Ti 掺杂制备高光电化学性能的 Fe_2O_3 光阳极

万丽娟[1,2]，张　丽[1]，杨　明[3]
(1. 南京交通职业技术学院，南京 211188；2. 江苏省交通节能减排工程技术研究中心，南京 211188；
3. 东南大学交通学院，南京 210096)

摘　要：通过金属有机物分解的方法合成了 Ti 掺杂 Fe_2O_3 光阳极. 通过 XRD、紫外—可见吸收光谱、X 射线光电子能谱(XPS)、扫描电镜(SEM)对 Fe_2O_3 光阳极进行表征，并对 Fe_2O_3 光阳极进行了光电化学表征. 为了提高 Ti 掺杂 Fe_2O_3 光阳极的光电性能，对 Ti 掺杂 Fe_2O_3 光阳极的 Ti 掺杂浓度进行了优化. 光电化学测试结果表明电化学表面处理能够提高 Ti 掺杂 Fe_2O_3 光阳极的光电化学性能. 说明 Ti 掺杂和电化学表面处理可以增加 Fe_2O_3 光阳极光电流. 基于 Mott-Schottky 曲线和电化学阻抗谱(EIS)分析了 Fe_2O_3 光阳极光电流增加的机理.

关键词：氧化铁；Ti 掺杂；光阳极
中图分类号：O643.3　　**文献标识码**：A　　**文章编号**：0490-6756(2018)05-1083-08

Synthesis of Fe_2O_3 photoanode with improved photoelectrochemical performance by surface electrochemical pretreatment and Ti-doping

WAN Li-Juan[1,2], *ZHANG Li*[1], *YANG Ming*[3]
(1. Nanjing Vocational Institute of Transport Technology, Nanjing 211188, China;
2. Jiangsu Engineering Technology Research Center for Energy Conservation and Emission Reduction of Transportation, Nanjing 211188, China; 3. School of Transportation, Southeast University, Nanjing 210096, China)

Abstract: Ti-doped Fe_2O_3 photoanode was obtained through metal-organic decomposition method. The physical and photophysical properties of the hematite photoanode were investigated by X-ray diffraction (XRD), UV-vis absorption spectroscopy, X-ray photoelectron spectroscopy (XPS) and scanning electron microscopy (SEM) and the photo-electrochemical performance was evaluated for the Ti-doped Fe_2O_3 photoanode. In terms of maximizing the photoelectrochemical performances of the Ti-doped Fe_2O_3 photoanodes, the doping concentration of titanium was optimized. The Ti-doped Fe_2O_3 photoanode exhibits improved photoelectrochemical performance after the electrochemical surface pretreatment. The photoelctrochemical response of hematite photoanode can be improved by both titanium doping and the electrochemical surface pretreatment. Based on the analysis of the Mott-Schottky plots and electrochemical impedance spectra (EIS), a possible mechanism was proposed to explain the reason for the enhancement of photocurrent.

Keywords: Hematite; Ti-doped; Photoanode

收稿日期：2017-12-18
基金项目：南京交通职业技术学院科研基金(JZ1704)；江苏省高校自然科学研究面上项目(16KJD610004)；国家自然科学基金(51208102)；南京交通职业技术学院高层次人才科研启动经费
作者简介：万丽娟(1978－)，女，山东章丘人，助理研究员，博士，研究方向为环境科学. E-mail:bartty_ym@163.com

1 Introduction

Semiconductor photoelectrochemical (PEC) or photocatalytic water splitting for hydrogen fuel production is a promising, clean and renewable strategy to solve environmental and energy issues through storing solar energy in the form of chemical bonds[1-3]. However, the low quantum efficiency for a photoelectrode poses a great challenge to water splitting by photocatalysis technique[4]. Some metal oxide materials with narrower band gaps have been studied intensively as photoanodes, such as WO_3, $BiVO_4$ and Fe_2O_3, due to their visible light response, low cost and fairly good stability[5-7]. Specifically, among the known transition metal oxide semiconductors, hematite (α-Fe_2O_3) has gained significant attraction due to the desired property of favorable band position and a narrow band gap of 2.0～2.2 eV, together with low cost, natural abundance, electrochemical stability and non-toxicity, however, due to a number of drawbacks and disadvantages such as slow charge carrier mobility, poor conductivity and fast electron-hole recombination rate, for α-Fe_2O_3 photoelectrodes, the reported water splitting efficiencies are much lower than the theoretical maximum efficiency[8]. Thus, in current research, there is a strong motivation to improve its electronic transport properties in this material by reducing the electron-hole recombination.

Doping with ions is one desirable approach to reduce the electron-hole recombination for the improved conduction by impurities through introducing charge compensation with parent ions[9]. Dopants were in general found to significantly alter the physical and electronic properties of hematite, thus, it is now common for substitutional doping of α-Fe_2O_3 and both isovalent and heterovalent atoms have been used such as Ti[10], Sn[11], W[12], and Zn[13] to reduce the electron-hole recombination rate and improve the PEC performance. Therefore, doping with Ti can improve the carrier concentration and the separation of photogenerated carriers[10], and through optimizing the doping concentration, the photoelectrochemical performances of α-Fe_2O_3 photoelectrodes doped with Ti may be improved.

A suitable synthesis technique which should be cheap, simple and easy to dope is also crucial for photoelectrode materials to realize the high PEC performance with the application in a large scale. Up to now, various synthesis techniques have been used to prepare hematite photoelectrodes, such as pulsed laser deposition (PLD)[14], atomic layer deposition (ALD)[15], chemical vapor deposition (CVD) techniques[16], spray-pyrolysis deposition (SPD) method[17], sol-gel route[18], hydrothermal method[19], electrodeposition[20], metal-organic decomposition method[21], (ultrasonic spray pyrolysis) USP[22] and *etc*. Among the synthesis techniques, metal-organic decomposition method which eases doping and good crystallinity is a facile method to prepare hematite photoelectrodes with high photoelectrochemical performance.

A number of approaches have also been adopted and shown to improve the photoelectrochemical performance, such as nanostructuring[23] and surface modification[24]. Recently, the surface pretreatment by electrochemical cyclic voltammetry (CV) is expected as a universal way to increase the photoelectrochemical performances of the photoelectrode, which has been reported to remove the surface recombination center[25, 26]. However, through the electrochemical surface pretreatment, the reports regarding the improvement of the photocurrent of Ti-doped hematite photoanodes prepared by metal-organic decomposition method are rare. In the present study, Ti-doped hematite photoanode was prepared via metal-organic decomposition method. The doping concentration was optimized in terms of maximizing the photoelectrochemical performances of the hematite photoanodes. The Ti-doped hematite photoanode by the electrochemical surface pretreatment exhibits improved photoelectrochemical performance and the possible mechanism was also discussed.

2 Experimental

2.1 Materials

The starting materials utilized are $Fe(NO_3)_3 \cdot 9H_2O$, tetrabutyl titanate, acetylacetone and ethanol (analysis purity grade, Sinopharm Chemical Reagent Co. Ltd.).

2.2 Synthesis of Ti-doped Fe_2O_3 photoanode

Hematite photoelectrodes were fabricated by metal-organic decomposition method. $Fe(NO_3)_3 \cdot 9H_2O$ in acetylacetone (0.1 mol $\cdot$ L^{-1}) was used as precursor solution. 70 ℃ of the precursor solution was dropped onto fluorine-doped tin oxide (FTO) substrates (2 cm × 1 cm). The solutions were dried in air, after which half of the coating was cleaned by ethanol to expose the conductive FTO substrate for subsequent testing. The prepared samples were then calcined at 700 ℃ for 15 minutes to form hematite films. To prepare for titanium doped hematite thin film photoelectrodes, we added different amount of tetrabutyl titanate in acetylacetone (0.04 mol $\cdot$ L^{-1}) solution into the $Fe(NO_3)_3 \cdot 9H_2O$ acetylacetone solution to produce different doping concentrations.

2.3 Characterization

Crystallinity of the products was identified by X-ray diffraction (XRD, Shimadzu 6000 X-ray diffractometer) with Cu Kα radiation ($\lambda = 0.154$ nm) and a scan rate of 10 ° $\cdot$ min^{-1}. The light absorption was obtained by measuring the transmittance using Ultraviolet visible (UV-vis) spectrophotometer with an integrating sphere (Lambda 750S, Perkin-Elmer) and the absorption spectra were obtained using the Kubelka-Munk method. The morphologies of the hematite films were observed using field emission scanning electron microscopy (FESEM, JEOL JSM-7600F) with an electron accelerating voltage of 5 kV. The chemical state of Fe was investigated by X-ray photoelectron spectroscopy (XPS, Omicron EA125). The binding energy was calibrated by C1s (284.6 eV).

2.4 Photoelectrochemical (PEC) measurements

Photoelectrochemical measurements were performed using a threeelectrode configuration (PCI4/300™ potentiostat with PHE200™ software, Gamry Electronic Instruments, Inc.) in a standard three-electrode configuration coupled with the sample films as the working electrode, an Ag/AgCl electrode as the reference electrode and a high purity Pt foil as the counter electrode. The photocurrents of water oxidation were measured in 1 M KOH aqueous solution with a scan rate of 30 mV $\cdot$ s^{-1}. The electrochemical pretreatment was carried out as follows before the photoelectrochemical properties of the samples were measured[26]. The as-prepared sample was scanned by cyclic voltammetry for 30 cycles in 1 M KOH in the dark. The cyclic voltammetry scans were performed at the scan speed of 20 mV $\cdot$ s^{-1} and with threshold reduction potential (−1.1 V). A solar simulator (HAL-320, Asahi Spectra Co., Ltd.) with power intensity of 100 mW $\cdot$ cm^{-2} was used as light source for photoelectrochemical measurement. The samples were illuminated from the front side (electrolyte/semiconductor interface). The mask-off irradiated area was 0.28 cm^2.

Electrochemical impedance spectroscopy (EIS) measurements were carried out under AM 1.5G solar simulator illumination (Oriel 92251A-1000) in 1 M KOH electrolyte at the applied potential of 0 V *vs.* Ag/AgCl using an AUTOLAB Potentiostat-Galvanostat (AUTOLAB PGSTAT302 N). The Mott-Schottky plots were also carried out using an AUTOLAB Potentiostat-Galvanostat (AUTOLAB PGSTAT302 N) at a fixed frequency of 1 kHz in 1 M KOH solution.

3 Results and discussion

The XRD patterns of the pure Fe_2O_3 and Ti-doped Fe_2O_3 films are shown in Fig. 1. From Fig. 1a, it shows that all peaks in the Fe_2O_3 samples agree well with the characteristic pattern of α-Fe_2O_3 structure (PDF # 33-0664). The crystal structure of the films after doped with Ti was also determined by XRD, as shown in Fig. 1b. From Fig. 1b, the XRD pattern characteristic of TiO_2 was not observed in Ti-doped Fe_2O_3 film, and no

noticeable peaks belonging to other phases appeared except the ones for the FTO (SnO_2) substrate, suggesting that titanium was probably incorporated with Fe_2O_3. The intense peaks of the XRD patterns indicate that the α-Fe_2O_3 products were well-crystallized. Moreover, the doping of Ti doesn't change the crystal structure. This demonstrates that Ti-doped hematite thin films can be successfully synthesized by the metal-organic decomposition method.

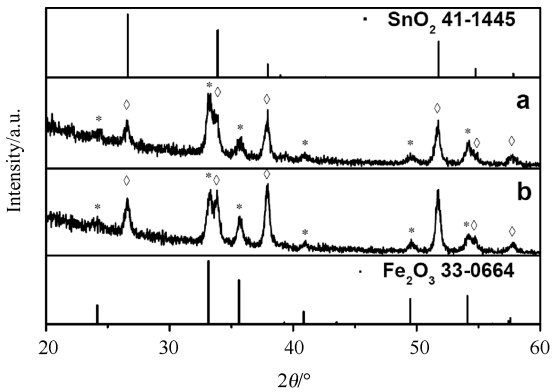

Fig. 1 XRD patterns of pure Fe_2O_3 film (a) and 2% Ti-doped Fe_2O_3 film (b) calcined at 700 ℃ for 15 min

The light absorptions of the pure Fe_2O_3 and Ti-doped Fe_2O_3 films samples were measured using UV-vis absorption spectroscopy, which are shown in Fig. 2. It is observed that all the Fe_2O_3 films possess good absorption to visible light. For hematite, the visible light absorption is due to the Fe^{3+} 3d-3d spin forbidden transition excitation[27]. The pure Fe_2O_3 film exhibits a broad absorption and Ti-doped Fe_2O_3 film exhibits a little higher absorption intensity compared with pure Fe_2O_3. Furthermore, the absorption edge of the Ti-doped Fe_2O_3 obviously shifts to a longer wavelength, which indicates that the band gap is narrowed by introducing Ti atoms. The absorption edges of the pure Fe_2O_3 and Ti-doped Fe_2O_3 sample occur at ca. 589 and 597 nm, and the optical band gaps of the samples are evaluated to be about 2.10 and 2.07 eV respectively. The reduction in the bandgap width from 2.10 to 2.07 eV can be attributed to the incorporation of Ti and such similar phenomenon has also been reported in other Ti-doped hematite materials[28]. Doping Ti may introduce additional more positive energy levels than the conduction band of Fe_2O_3, which facilitates electrons to be excited from valence band to conduction band[29].

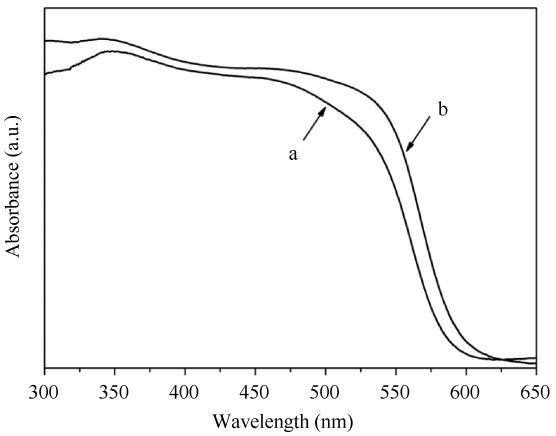

Fig. 2 The UV-vis absorption spectra of the pure Fe_2O_3 (a) and Ti-doped Fe_2O_3 (b)

XPS measurements were performed to analyze the oxidation state of Ti in the Ti-doped hematite films and the result is shown in Fig. 3. From Fig. 3, it shows that the Ti-doped α-Fe_2O_3 film shows clear Ti 2p peaks at 458.2 eV ($2p_{3/2}$) and 464.1 eV ($2p_{1/2}$). These Ti 2p peaks of Ti in the Ti-doped hematite films are consistent with Ti in a fully oxidized Ti^{4+} state[30]. Thus, after a high-temperature annealing process, it is expected that fully oxidized Ti^{4+} dopants exist in the hematite films.

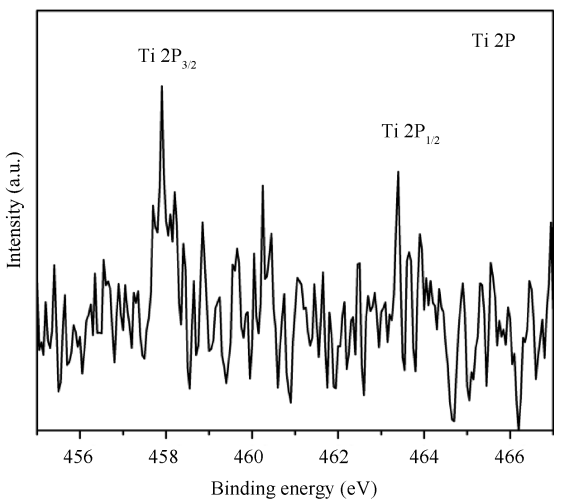

Fig. 3 High resolution XPS of Ti for the Ti-doped Fe_2O_3 photoelectrode

SEM image of the Ti-doped hematite film prepared by metal-organic decomposition method is shown in Fig. 4. The SEM image illustrates that the surface structure of Ti-doped hematite is in a compact film form. It is shown that the films exhibit a planar structure and due to the film shrinkage during calcinations, some cracks appear. Nevertheless, the film showed the strongly adhesive property to the FTO substrate even after scrapping action. For the surface morphology, no changes were observed after electrochemical treatment for Ti-doped hematite thin films.

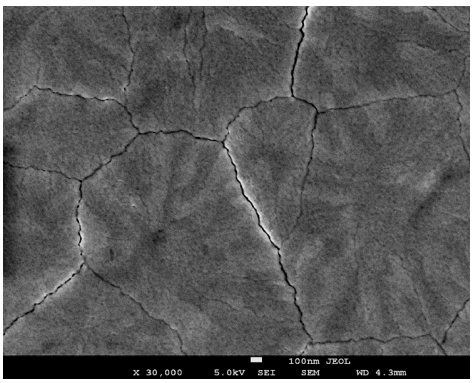

Fig. 4　SEM image of the surface of Ti-doped Fe_2O_3 film

Mott-Schottky plots of pristine and Ti-doped hematite samples were obtained to investigate the carrier density, which is shown in Fig. 5. From Fig. 5, electrons are the majority carriers as indicated by the positive Mott-Schottky slopes. The carrier density can be estimated using the following equation[21]:

$$N_d = (2/e_0\varepsilon\varepsilon_0)[d(1/C^2)/dV]^{-1} \quad (1)$$

where e_0 is the electron charge (1.60×10^{-19} C), ε is the dielectric constant of hematite (80), ε_0 is the permittivity of vacuum (8.85×10^{-12} F·m^{-1}), N_d is the donor density and V is the potential applied at the electrode. From the electrochemical impedance measured at each potential in the dark, capacitances were obtained. After the doping of titanium, the slope of hematite decreases which indicates the enhancement of carrier density. The corresponding carrier density is 3.51×10^{19} cm^{-3} for pristine hematite, while the calculated donor density of the Ti-doped hematite is 8.82×10^{20} cm^{-3}. The increased carrier (electron) density improves the conductivity which can facilitate the enhancement of charge separation efficiencies of Ti-doped hematite.

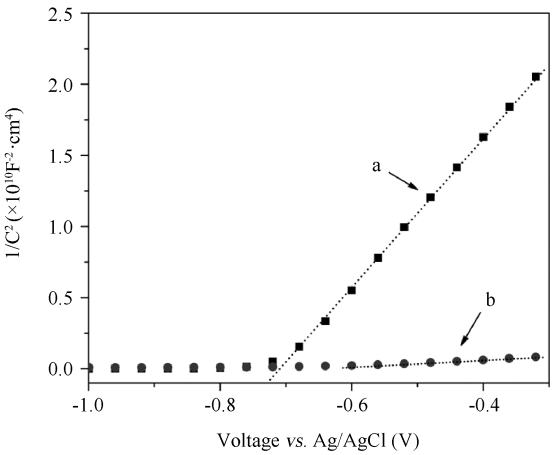

Fig. 5　Mott-Schottky plots of (a) pure and (b) Ti-doped hematite at a fixed frequency of 1 kHz in 1 M KOH aqueous solution

To investigate the charge transfer process, electrochemical impedance spectra (EIS) were recorded. EIS was performed under simulated solar illumination for reflecting the real situation of the charge transfer process of water oxidation. The Nyquist plots under 1 Sun simulated solar illumination are shown in Fig. 6. In the EIS, two semicircles are observed which are similar to those reported for hematite electrodes[31]. It has been reported that water is oxidized from surface trapped holes which are first trapped by the surface states while not directly from valence band holes[31]. A model was also proposed to analyze the EIS and is adopted in the current study. In the inset in Fig. 6, R_{trap} stands for the resistance of the surface states trapping holes; R_s stands for the total resistance from the external circuit; and R_{ss} stands for the surface charge transfer resistance in the equivalent circuit. The fitting results showed that the surface charge transfer resistance of pristine hematite was 24.40 kΩ. For Ti-doped hematite, the surface charge transfer resistance was 0.89 kΩ. Compared with that of pristine hematite, the decreased surface charge transfer resistance of Ti-doped hematite may be beneficial to improve the

photoelectrochemical performance.

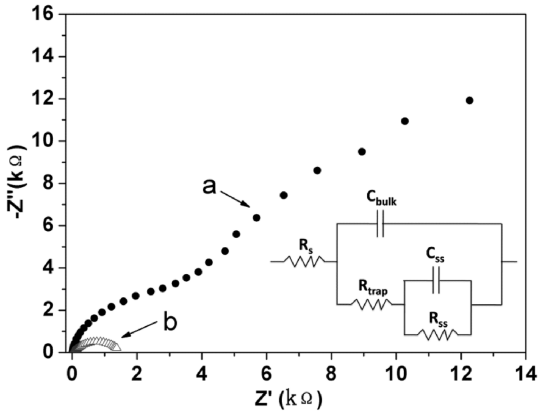

Fig. 6 Electrochemical impedance spectra (EIS) of (a) pure and (b) Ti-doped hematite at an applied potential of 0 V *vs.* Ag/AgCl in 1 M KOH electrolyte under simulated solar illumination. The inset is the equivalent circuit to simulate the EIS according to Klahr *et al.*'s work[27]. R_s represents the total resistance from the external circuit; C_{bulk} is the space charge capacitance of the bulk; R_{trap} is the resistance of the surface states trapping holes; C_{ss} is the surface state capacitance; R_{ss} is the charge transfer resistance of holes from the surface states to solution.

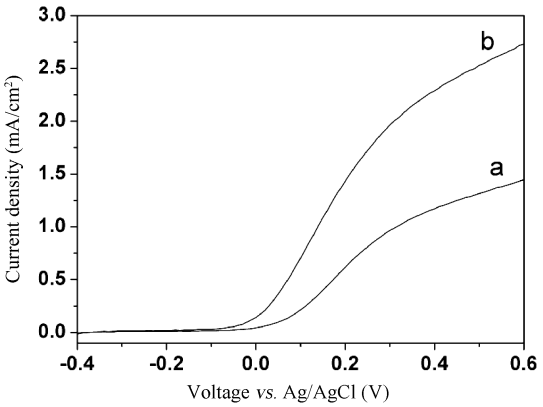

Fig. 7 Photocurrent curves of the Fe_2O_3 sample by 2% Ti-doped: a. before surface pretreatment; b. after surface pretreatment

The photocurrent curves of Ti-doped hematite before and after surface pretreatment samples are shown in Fig. 7. From Fig. 7, it is shown that the sample after the pretreatment shows the obvious enhancement of photocurrent compared with the Ti-doped hematite sample without electrochemical pretreatment. The electrochemical pretreatment make the photocurrent of Ti-doped hematite sample at 0.6 V *vs.* Ag/AgCl twice more than that of the sample without surface pretreatment. It has been previously reported that a favorable photohole transfer and a significant decrease of charge recombination can be induced by electrochemical reduction pretreatment which is physically associated with the partial transformation of hematite[26]. From the above results, it is proven that the electrochemical pretreatment is also a efficient method to improve the photocurrent of the Ti-doped hematite sample prepared by metal-organic decomposition method.

The photocurrent of Ti-doped hematite photoelectrodes may be improved through optimizing the doping concentration of titanium. The pure hematite sample and the samples doped with titanium prepared by metal-organic decomposition method and after the surface pretreatment are investigated. The photocurrent curves of the pure and Ti-doped hematite samples with different doping concentrations are shown in Fig. 8. As shown in Fig. 8, the photocurrent of the doped film shows a significant increase compared with the pure hematite film. The improved photoelectrochemical performance may come from a reduction in charge recombination by the enhanced electrical conductivity, which would lengthen the lifetime of charge carriers[32]. From Fig. 8, the result shows that when the doping concentration is increased from 1% to 2%, the photocurrent is obviously improved at potential higher than 0.1 V. The photocurrent of the Ti-doped hematite increases to about 1.2 times after the doping concentration of titanium is increased from 1% to 2% at potential of 0.6 V. The pronounced enhancement in PEC performance is supposed to be attributed to the increased donor density by Ti doping[33]. Due to the competition between charge transport and electron-hole recombination, the electron-hole recombination is also likely to be reduced by the enhanced electrical conductivity by Ti doping.[34] Thus, the increase of the photocurrent may be contributed to the increased donor density and the reduced electron-hole recombination induced by the doping of titanium. While compared with that of those samples with the Ti doping concentration of 1% or 2%, the photocurrent for the sample with the Ti do-

ping concentration of 3% is lower. That indicates that the increase of the recombination of photo-generated carriers may be induced by higher doping concentration and thus the photocurrent is decreased. The lower performance of the doped photoanode with higher Ti doping concentration may result from a lower hole current and lower charge-transfer efficiency[35], furthermore, doping in higher concentration can decrease the width of the depletion layer and thus enhance carrier recombination[36].

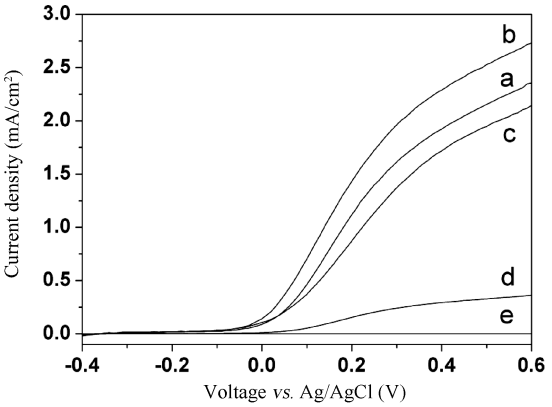

Fig. 8　Photocurrent curves of the Ti-doped Fe_2O_3 samples with different doping concentrations: a. 1% Ti; b. 2% Ti; c. 3% Ti; pure Fe_2O_3 sample under light irradiation (d) and in dark (e)

4　Conclusions

In summary, Ti-doped hematite thin films were deposited by metal-organic decomposition method. 2% Ti-doped hematite sample after the electrochemical surface pretreatment showed the highest photoelectrochemical performance. Both titanium doping and the electrochemical surface pretreatment can improve the photoelctrochemical response of the hematite thin films, which is attributed to the increased donor density and the reduced electron-hole recombination.

References:

[1] Grätzel M. Photoelectrochemical cells [J]. Nature, 2001, 414: 338.

[2] Li Z S, Luo W J, Zhang M L, *et al*. Photoelectrochemical cells for solar hydrogen production: current state of promising photoelectrodes, methods to improve their properties, and outlook [J]. Energy Environ Sci, 2013, 6: 347.

[3] Zhou L L. Synthesis of BiOBr/I nanocomposites and photocatalytic activities to organic compounds [J]. J Sichuan Univ: Nat Sci Ed(四川大学学报：自然科学版), 2015, 52: 370(in Chinese)

[4] Rao P M, Cai L, Liu C, *et al*. Simultaneously efficient light absorption and charge separation in $WO_3/BiVO_4$ core/shell nanowire photoanode for photoelectrochemical water oxidation [J]. Nano Lett, 2014, 14: 1099.

[5] Cesar I, Kay A, Gonzalez Martinez J A, *et al*. Translucent thin film Fe_2O_3 photoanodes for efficient water splitting by sunlight: nanostructure-directing effect of Si-doping [J]. J Am Chem Soc, 2006, 128: 4582.

[6] Luo W J, Yang Z S, Li Z S, *et al*. Solar hydrogen generation from seawater with a modified $BiVO_4$ photoanode [J]. Energy Environ Sci, 2011, 4: 4046.

[7] Santato C, Odziemkowski M, Ulmann M, *et al*. Crystallographically oriented mesoporous WO_3 films: synthesis, characterization, and applications [J]. J Am Chem Soc, 2001, 123: 10639.

[8] Glasscock J A, Barnes P R F, Plumb I C, *et al*. Enhancement of photoelectrochemical hydrogen production from hematite thin films by the introduction of Ti and Si [J]. J Phys Chem C, 2007, 111: 16477.

[9] Liao P, Toroker M C, Carter E A. Electron transport in pure and doped hematite [J]. Nano Lett, 2011, 11: 1775.

[10] Wang G, Ling Y, Wheeler D A, *et al*. Facile synthesis of highly photoactive α-Fe_2O_3-based films for water oxidation [J]. Nano Lett, 2011, 11: 3503.

[11] Hahn N T, Mullins C B. Photoelectrochemical performance of nanostructured Ti and Sn-doped α-Fe_2O_3 photoanodes [J]. Chem Mater, 2010, 22: 6474.

[12] Shen S, Kronawitter C X, Jiang J, *et al*. Surface tuning for promoted charge transfer in hematite nanorod arrays as water-splitting photoanodes [J]. Nano Res, 2012, 5: 327.

[13] Ingler W B, Baltrus J P, Khan S U M. Photoresponse of p-type zinc-doped iron(III) oxide thin films [J]. J Am Chem Soc, 2004, 126: 10238.

[14] Kronawitter C X, Mao S S, Antoun B R. Doped, porous iron oxide films and their optical functions and anodic photocurrents for solar water splitting [J]. Appl Phys Lett, 2011, 98: 092108.

[15] Zandi O, Klahr B M, Hamann T W. Highly photoactive Ti-doped α-Fe_2O_3 thin film electrodes: resurrection of the dead layer [J]. Energy Environ Sci,

2013, 6: 634.

[16] Zhang P, Kleiman-Shwarsctein A, Hu Y S, *et al*. Oriented Ti doped hematite thin film as active photoanodes synthesized by facile APCVD [J]. Energy Environ Sci, 2011, 4: 1020.

[17] Kumari S, Singh A P, Sonal, *et al*. Spray pyrolytically deposited nanoporous Ti^{4+} doped hematite thin films for efficient photoelectrochemical splitting of water [J]. Int J Hydrogen Energy, 2010, 35: 3985.

[18] Lian X, Yang X, Liu S, *et al*. Enhanced photoelectrochemical performance of Ti-doped hematite thin films prepared by the sol-gel method [J]. Appl Surf Sci, 2012, 258: 2307.

[19] Yang T Y, Kang H Y, Jin K, *et al*. An iron oxide photoanode with hierarchical nanostructure for efficient water oxidation [J]. J Mater Chem A, 2014, 2: 2297.

[20] Wang L, Lee C Y, Schmuki P. Ti and Sn co-doped anodic α-Fe_2O_3 films for efficient water splitting [J]. Electrochem Commun, 2013, 30: 21.

[21] Zhao X, Feng J Y, Chen S, *et al*. New insight into the roles of oxygen vacancies in hematite for solar water splitting [J]. Phys Chem Chem Phys, 2017, 19: 1074.

[22] Zhang M, Luo W, Li Z S, *et al*. Improved photoelectrochemical responses of Si and Ti codoped α-Fe_2O_3 photoanode films [J]. Appl Phys Lett, 2010, 97: 042105.

[23] Hamann T W. Splitting water with rust: hematite photoelectrochemistry [J]. Dalton Trans, 2012, 41: 7830.

[24] Klahr B, Gimenez S, Fabregat-Santiago F, *et al*. Photoelectrochemical and impedance spectroscopic investigation of water oxidation with "Co-Pi"-coated hematite electrodes [J]. J Am Chem Soc, 2012, 134: 16693.

[25] Luo W J, Li Z S, Yu T, *et al*. Effects of surface electrochemical pretreatment on the photoelectrochemical performance of Mo-doped $BiVO_4$ [J]. J Phys Chem C, 2012, 116: 5076.

[26] Shangguan P P, Tong S P, Li H L, *et al*. Enhanced photoelectrochemical oxidation of water over undoped and Ti-doped α-Fe_2O_3 electrodes by electrochemical reduction pretreatment [J]. RSC Adv, 2013, 3: 10163.

[27] Liu Y, Wang D P, Yu Y X, *et al*. Preparation and photoelectrochemical properties of functional carbon nanotubes and Ti co-doped Fe_2O_3 thin films [J]. Int J Hydrogen Energ, 2012, 37: 9566.

[28] Xie X, Li K, Zhang W D. Photoelectrochemical properties of Ti-doped hematite nanosheet arrays decorated with CdS nanoparticles [J]. RSC Adv, 2016, 6: 74234.

[29] Thimsen E, Biswas S, Lo C S, *et al*. Predicting the band structure of mixed transition metal oxides: theory and experiment [J]. J Phys Chem C, 2009, 113: 2014.

[30] Carley A F, Chalker P R, Riviere J C, *et al*. The identification and characterisation of mixed oxidation states at oxidised titanium surfaces by analysis of X-ray photoelectron spectra [J]. J Chem Soc: Faraday Trans, 1987, 83: 351.

[31] Klahr B, Gimenez S, Fabregat-Santiago F, *et al*. Water oxidation at hematite photoelectrodes: The role of surface states [J]. J Am Chem Soc, 2012, 134: 4294.

[32] Meng X Y, Qin G W, Li S, *et al*. Enhanced photoelectrochemical activity for Cu and Ti doped hematite: The first principles calculations [J]. Appl Phys Lett, 2011, 98: 112104.

[33] Cheng W, He J, Sun Z, *et al*. Ni-doped overlayer hematite nanotube: a highly photoactive architecture for utilization of visible light [J]. J Phys Chem C, 2012, 116: 24060.

[34] Shen S H, Kronawitter C X, Wheeler D A, *et al*. Physical and photoelectrochemical characterization of Ti-doped hematite photoanodes prepared by solution growth [J]. J Mater Chem A, 2013, 1: 14498.

[35] Malviya K D, Klotz D, Dotan H, *et al*. Influence of Ti doping levels on the photoelectrochemical properties of thin-film hematite (α-Fe_2O_3) photoanodes [J]. J Phys Chem C, 2017, 121: 4206.

[36] Karakitsou K E, Verykios, X E. Effects of altervalent cation, doping of TiO_2 on its performance as a photocatalyst for water cleavage [J]. J Phys Chem, 1993, 97: 1184.

引用本文格式:

中 文:万丽娟, 张丽, 杨明. 电化学表面处理和 Ti 掺杂制备高光电化学性能的 Fe_2O_3 光阳极[J]. 四川大学学报: 自然科学版, 2018, 55: 1083.

英 文: Wan L J, Zhang L, Yang M. Synthesis of Fe_2O_3 photoanode with improved photoelectrochemical performance by surface electrochemical pretreatment and Ti-doping [J]. J Sichuan Univ: Nat Sci Ed, 2018, 55: 1083.